Measurement of the electric polarizability of sodium with an atom interferometer

Christopher R. Ekstrom,[1] Jörg Schmiedmayer,[1,2] Michael S. Chapman,[1] Troy D. Hammond,[1] and David E. Pritchard[1]
[1]*Department of Physics and Research Laboratory of Electronics, Massachusetts Institute of Technology, Cambridge, Massachusetts 02139*
[2]*Institut für Experimentalphysik, Universität Innsbruck, A-6020 Innsbruck, Austria*
(Received 3 January 1995)

We have constructed an atom interferometer with interfering beams that are physically isolated by a metal foil. By applying an interaction to one of the two interfering beams, we can measure ground-state energy shifts with a spectroscopic precision of 6.6×10^{-14} eV/$\sqrt{\text{min}}$, or 16 Hz/$\sqrt{\text{min}}$. Applying an electric field to one beam of the interferometer, we have measured the phase shift induced from the quadratic Stark effect. By analyzing these phase shifts, we have determined the ground-state polarizability of sodium, with much improved accuracy, to be $24.11(6)_{\text{statistical}}(6)_{\text{systematic}}\times10^{-24}$ cm^3.

PACS number(s): 03.75.Dg, 32.10.Dk, 07.60.Ly

I. INTRODUCTION

Recently, there have been several atomic interference experiments culminating in the demonstration of atom interferometers that are now beginning to be used as experimental tools in the field of atomic physics [1–7]. We report in this paper an atom interferometer in which the two interfering components of each atom's wave (henceforth called beams) are physically isolated, permitting the controlled application of different interactions to the two beams. This development makes atom interferometers, like separated beam neutron interferometers [8], ideal instruments with which to test fundamental predictions of quantum mechanics.

An important application of such interferometers is the measurement of ground-state atomic properties and interactions where atomic beam resonance techniques [9] are not applicable because all the sublevels are shifted similarly. Having the two interfering beams physically separated allows absolute measurements of shifts in the ground-state energy with spectroscopic precision by measuring the phase shift of the atomic wave function when the interaction is applied to one beam. This gives a large increase in sensitivity compared to the standard technique of measuring ground-state interactions by deflection in a potential gradient [10].

We have used this technique to perform a 0.3% measurement of the polarizability of sodium. This is an order-of-magnitude increase in accuracy relative to any of the competing techniques for measuring atomic polarizability for condensable species [11]. Our experiment is more accurate than all but one of the calculations [12–19] made since the previous measurements [10,20] and will allow much better discrimination among the various theories. Knowledge of atomic polarizability enables prediction of many other properties of atomic systems including the dielectric constant and index of refraction, the van der Waals constant between two polarizable systems, and the Rayleigh scattering cross section. In addition, our measurement allows the separate extraction of polarizabilities of ground and excited states if combined with measurements of the differences of ground- and excited-state polarizabilities, which can be made with spectroscopic techniques [21,22] or interferometric techniques in which the interfering paths are not spatially isolated [6].

II. EXPERIMENTAL APPARATUS

Our interferometer is a three-grating Mach-Zender interferometer [23] (Fig. 1) that has been modified by the incorporation of an interaction region containing a metal foil to physically isolate the two beams. The experimental apparatus has been considerably improved since our first demonstration experiment [2] and has been described in detail elsewhere [24]. In the experiment described here, we use a sodium beam with a mean velocity of 1050 m/s, corresponding to a de Broglie wavelength of 0.17 Å, with a typical velocity width of 4% rms. We now use 200-nm-period nanofabricated transmission gratings [25] that separate the centers of the beams by 55 μm at the position of the second grating, where the full width at half maximum of each beam is 40 μm.

The interaction region consists of a stretched metal foil held symmetrically between two side electrodes. The foil

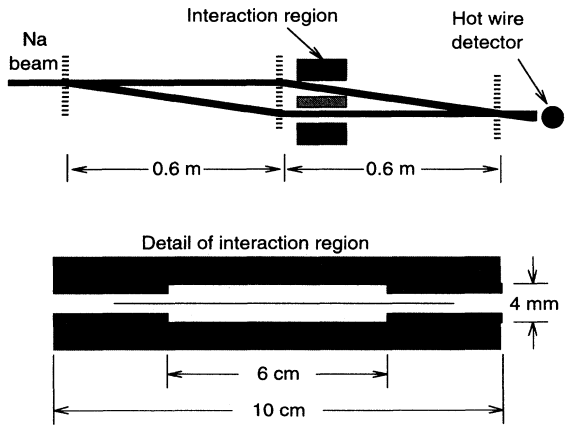

FIG. 1. Schematic of our interferometer and interaction region. Vertical dashed lines are 200-nm-period diffraction gratings. The detail of the interaction region shows the 10-μm copper foil suspended between the side plates. The guard electrodes are indicated in black at both ends.

 ©1995 The American Physical Society

is spaced from the side plates with insulating 2-mm-thick precision ground alumina spacers (Fig. 2). The septum must be thin and very flat (<30 μm) over the whole length of about 10 cm to fit between the two interfering beams, which are separated by only 55 μm in the interferometer. This is achieved by cutting the foil into a "butterfly" shape chosen to pull all wrinkles in the foil out to the area that will not be used in the final interaction region (Fig. 3). The foil is then carefully stretched flat and clamped between the spacers, side plates, and a mounting clamp. We have used various materials successfully including a 10-μm-thick copper foil and 12-μm-thick metalized Mylar.

The interaction region is mounted behind the second grating on a stack of manipulators. These provide transverse translation to move the foil in and out of the beam line, rotation about the beam axis to align the foil to the beam over its full height, and rotation about the vertical axis to make the plane of the foil parallel to the atomic beam. A typical 10-cm-long septum, aligned to the atomic beam, casts a shadow on the detector that corresponds to a 20–30-μm-wide septum. This is wider than the nominal 10-μm foil thickness due to remaining imperfections once it is stretched. With the septum positioned between the beams of the interferometer, we have observed fringes with 35% contrast and an interference amplitude of more than 800 counts/s (Fig. 4).

This conducting, physical barrier between the separated beams allows the application of different interactions to the two paths in the interferometer, and measurements of the resulting phase shifts. The sensitivity of this phase-shift measurement is set by the interaction time. The intrinsic linewidth is 10 kHz with our 1050-m/s beam and 10-cm-long interaction region. We can determine the phase of the interference pattern with a precision of 10 mrad in 1 min, which corresponds to a sensitivity to energy shifts of roughly 6.6×10^{-14} eV/$\sqrt{\text{min}}$, or 16 Hz/$\sqrt{\text{min}}$.

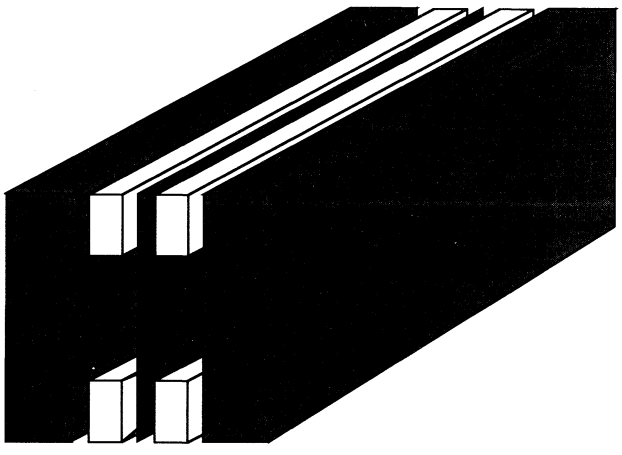

FIG. 2. Expanded view of the interaction region. The foil is black. The insulating alumina spacers are shown in white, and the aluminum side plates are gray. The split atomic beams of the interferometer enter from the front (lower left) and pass on either side of the foil.

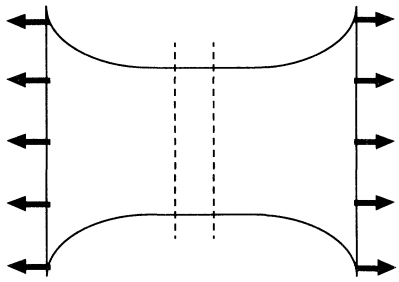

FIG. 3. The foil into a "butterfly" shape is stretched from both sides to remove wrinkles. The area inside the dotted lines is used in the final interaction region.

III. EXPERIMENTAL METHOD

When an atom moves in a potential $U(x)$, the phase evolution of the wave function can be written within the JWKB approximation as $\psi(x)\propto e^{i\int k(x)dx}$, with $k(x)=(1/\hbar)\sqrt{2m[E-U(x)]}$ and the integration performed along the classical path. Applying a potential to one of the two beams in our interferometer, the resulting phase difference between the two beams is

$$\Delta\varphi(k)=\int k(x)dx-\int k_0dx\approx-\frac{1}{\hbar v}\int U(x)dx\ . \qquad (1)$$

The approximation is valid when $U(x)\ll E$ [$U(x)\approx10^{-8}E$ in our experiment].

In this experiment we apply a uniform electric field $\mathcal{E}$ to one of the separated atomic beams, shifting its energy by the Stark potential $U=-\alpha\mathcal{E}^2/2$. The scalar ground-state polarizability is determined from the phase shift of the interference pattern using Eq. (1) with $\mathcal{E}=V/D$, yielding

$$\alpha=\left[\frac{\Delta\varphi_{\text{Stark}}}{V^2}\right]\left[\frac{D^2}{L_{\text{eff}}}\right](2\hbar v)\ , \qquad (2)$$

where L_{eff} is the effective interaction region length, V is the voltage applied to one side of the interaction region across a distance D, the spacer width, and v is the mean velocity of the atomic beam. We now discuss the measurement and associated statistical and systematic errors of the three factors in Eq. (2).

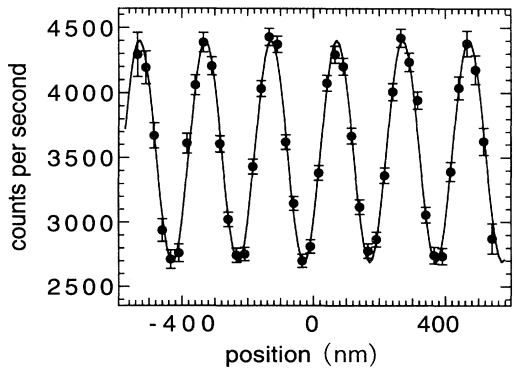

FIG. 4. Interference pattern from 40 s of data (1 per point). A constant background of 200 cps has been subtracted.

To measure the first factor in Eq. (2) ($\Delta\varphi_{\text{Stark}}/V^2$), we fit the phase shifts from several different voltages to a quadratic function of voltage (Fig. 5). The phase for a given voltage is measured with respect to the phase with no voltage applied. This zero voltage reference phase typically drifts 1 rad/h, with short term (30 s) rms fluctuations as large as 150 mrad. To correct for these drifts and fluctuations, we take frequent measurements of the reference phase. In the fit, the quadratic term has a statistical uncertainty, typically 0.2%, due to both counting statistics and phase fluctuations. We observed no statistically significant variation with the sign of the voltage, indicating the absence of significant contact potentials.

The second factor in Eq. (2) is determined by the geometry of the interaction region. The electric fields of the interaction region are calculated numerically using standard relaxation methods, and the results are parametrized by an effective length L_{eff} defined as

$$\left[\frac{V}{D}\right]^2 L_{\text{eff}} \equiv \int \mathcal{E}^2 dx \ . \tag{3}$$

We performed polarizability measurements with three different interaction regions, none of which had more than a 3% difference between L_{eff} and the respective physical length (Fig. 6). The first and second interaction regions had foils with lengths of 10 cm and 7 cm but no guard electrodes. The third interaction region had guard electrodes located at the ends of the side plates and spaced 6 cm apart (Fig. 1), which were held at the same potential as the foil to minimize the fringing fields. These different electric-field geometries gave consistent results for the polarizability within errors. The final result was dominated by the interaction region with guard electrodes because its better characterized electric fields contributed only 0.1% systematic error to L_{eff}.

The spacer thicknesses D have been measured to 0.05% with a dial indicator calibrated with precision gauge blocks. Differences in the individual spacer thicknesses produced an asymmetry in the interaction region, which we measured to be 0.1(1)%. This asymmetry was independently confirmed in the interferometer by measuring the phase shift when a voltage is applied to the septum and guard electrodes with the side plates held at ground, yielding 0.17(5)% asymmetry. After correcting for the measured asymmetry, there was no statistically significant difference (0.2%) in the polarizability between the left and right sides of the interaction region. The combined effect of dimensional uncertainties of L_{eff} and D thus contribute a systematic error of less than 0.2% in $\int \mathcal{E}^2 dx$.

The third factor in Eq. (2) is the velocity of the sodium beam. The mean velocity was determined to 0.15% from

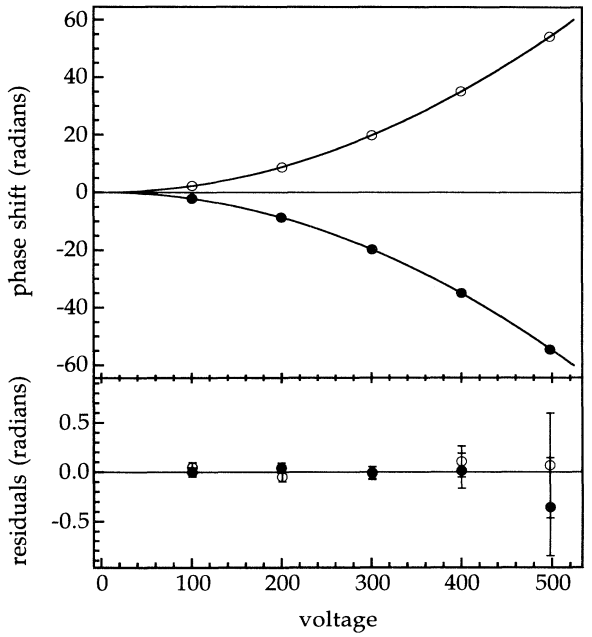

FIG. 5. Phase shift of the interference pattern as a function of voltage applied (in volts) to the left (open circles) or right (filled circles) side of the interaction region. The fit is to a quadratic and the residuals are shown in the lower graph.

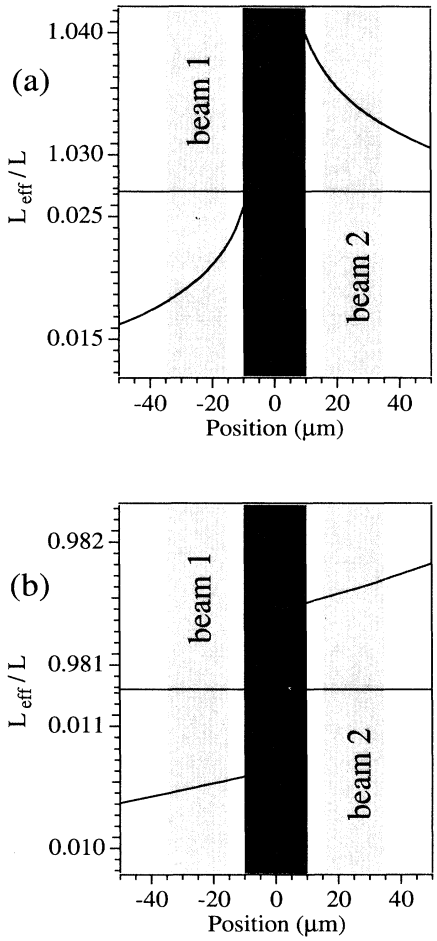

FIG. 6. Calculated values of L_{eff} as a function of distance from the septum (black) for interaction regions (a) without any guard electrodes and (b) with guard electrodes. The gray areas labeled beam 1 and beam 2 show the approximate paths of the two atom beams with respect to the septum. Here, the voltage is applied to the side containing beam 2.

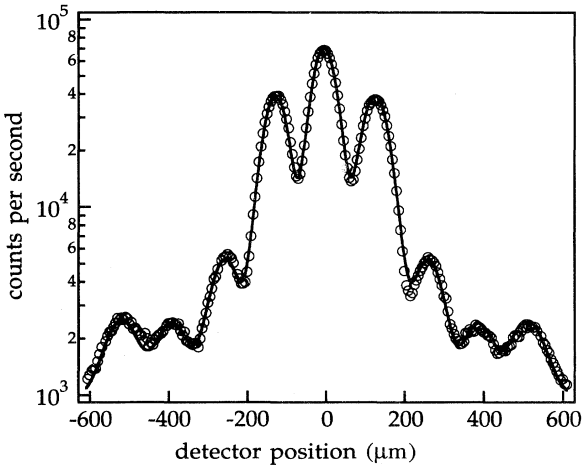

FIG. 7. Diffraction pattern of sodium atoms from a 200-nm period grating. The solid line is calculated for a grating with average open fraction of 39.5%. The fit yields a mean velocity of 1040(2) m/s, $\lambda_{dB}=0.167$ Å, and a rms velocity width of 3.7(4)%.

a fit to the diffraction pattern produced by the first grating (period 200±0.1 nm) with the second and third gratings removed (Fig. 7). The velocity is determined from the diffraction angle by

$$\theta_{\text{diff}}=\frac{\lambda_{\text{Na}}}{d}=\frac{h}{mv}\frac{1}{d}\ , \tag{4}$$

where d is the grating period and $\lambda_{\text{Na}}=2\pi/k_0$ is the de Broglie wavelength. The rms width of the velocity distribution is also determined by this fit.

IV. SYSTEMATIC ERRORS

As we are performing a precision measurement, it is necessary to quantify and deal with possible systematic shifts and errors. In our interferometer and interaction region, most of the systematic effects come from the velocity distribution of our atomic beam and effects that alter this velocity distribution.

In the limit of a monochromatic atomic beam, we have measured all the quantities in Eq. (2) necessary to determine the polarizability. The finite velocity distribution of our beam complicates this simple analysis. The rms width of the velocity distribution varies between 3% and 5% and depends primarily on the carrier gas pressure and nozzle diameter of the seeded supersonic source. We can measure this width to 10% from the broadening of the high-order peaks in the diffraction pattern or from the coherence length of our beam [26]. The two determinations are consistent.

We first consider the results of averaging over an arbitrary velocity distribution $P(v)$, which will affect the measured phase of the interference pattern. The measured phase will not be $\varphi(\bar{v})$, where $\bar{v}$ is the mean velocity, but will be given by

$$\varphi_{\text{measured}}=\arctan\left[\frac{\int P(v)\sin\varphi(v)dv}{\int P(v)\cos\varphi(v)dv}\right]\ . \tag{5}$$

The difference between $\varphi_{\text{measured}}$ and $\varphi(\bar{v})$ depends primarily on the mean velocity and, to a lesser extent, on the velocity width. It is only weakly dependent on the exact form of the distribution. We use a Gaussian model function (instead of a more realistic v^3 weighted Gaussian) for calculational convenience as there is no difference between the results at the 0.01% level. A similar velocity average is applied to the fit of the diffraction pattern, producing a 0.15% correction to the mean velocity found from the locations of the diffraction peaks using Eq. (4).

Because we use diffractive beam splitters in our interferometer, atoms from different velocity classes travel on different paths and may be detected differently. Therefore, systematic errors can occur because the velocity distribution contributing to the interference pattern differs from the velocity distribution of all atoms coming from the supersonic source, which is determined from the diffraction pattern.

In our experiment, there are two sources of this type of systematic velocity distribution change. One is the velocity-selective blocking of atoms by the septum. Faster atoms have a smaller diffraction angle and, therefore, a larger chance of being blocked by the septum. The second is velocity-selective detection of atoms. The same correlation between velocity and diffraction angle results in a correlation between the detector position and the velocity distribution of the atoms that are detected. These systematic effects were modeled with a ray-tracing algorithm. The calculation was performed for a variety of septum and detector positions, allowing us to find corrections to the measured phase shift and contrast reduction for each experimental configuration.

We measured the polarizability at many positions of the interaction region within the interferometer. These measurements agreed with the predictions from the model (Fig. 8), showing no variation in the polarizability at the 0.1% level for excursions of the septum that reduce

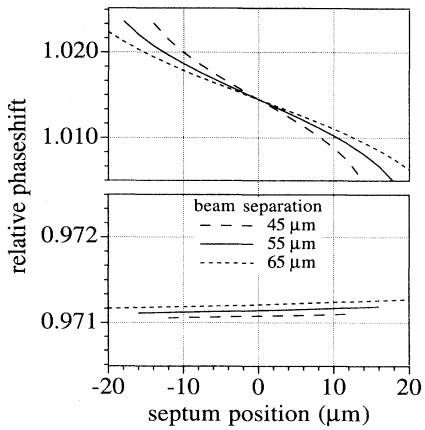

FIG. 8. Calculated relative phase shift as a function of the septum position between the two interfering atom beams for an interaction region without any guard electrodes (top) and with guard electrodes (bottom). A relative phase shift of 1 would be measured for a monochromatic beam and an interaction region with $L_{\text{eff}}=L$. Results are shown for three different beam separations, centered about our typical value of 55 μm.

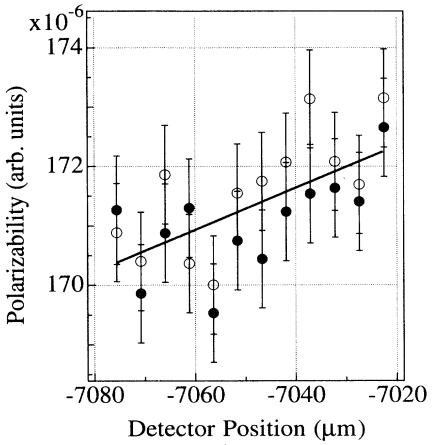

FIG. 9. Polarizability data as a function of the detector position. The data are the coefficients from a quadratic fit of the phase shift vs the applied voltage and are related to the polarizability by Eq. (2). The data are for voltages applied to the left (open circles) and right (filled circles) sides of the interaction region. The straight line is a fit to all the data and shows a 0.021% variation of measured polarizability per micrometer change in detector position.

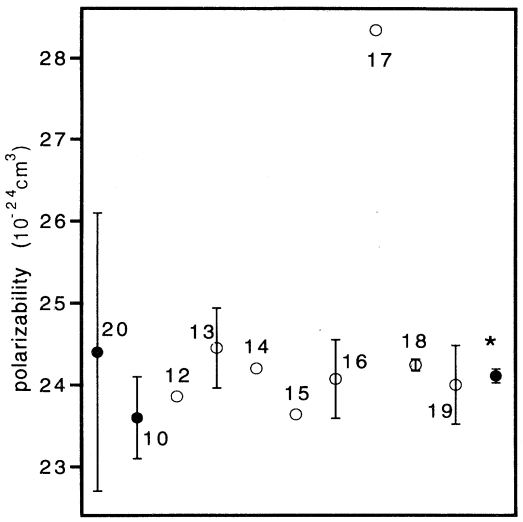

FIG. 10. Recent theoretical calculations (open circles) and experimental measurements (closed circles) of the electric polarizability of sodium. The values appear in chronological order and are labeled with the appropriate reference number. The symbol * indicates this work.

the contrast to 50% of its peak value. This systematic is insignificant at our level of precision and required no correction.

We also measured the polarizability at several detector positions. These data show a correlation between measured polarizability and detector position of 0.021% per micrometer (Fig. 9), agreeing within errors to the model calculations. The resulting corrections of about 0.4%, which include the velocity average of Eq. (5), introduced a systematic uncertainty of 0.15% in our determination of the polarizability.

V. RESULTS

We find the Stark shift of the ground state of sodium to be 40.56(10)(10) kHz/(kV/cm)^2, which corresponds to an electric polarizability of $\alpha=24.11(6)(6)\times10^{-24}$ cm^3 where the first error is statistical and the second is systematic. The systematic error is dominated by uncertainties in the geometry of the interaction region, but also includes other geometric factors common to all measurements such as uncertainty in the grating period (0.05%) and apparatus dimensions, which are used to find the velocity. Our statistical error is dominated by uncertainty in the determination of our velocity distribution, the short term stability of the phase reference in our experiment, and to a lesser extent by counting statistics.

The best previous direct measurement of the polarizability of sodium gave $24.4(1.7)\times10^{-24}$ cm^3 [20], a 7% result. The currently accepted value $23.6(5)\times10^{-24}$ cm^3, with a 2% uncertainty [10], comes from a measurement of the polarizability with respect to that of the $2\,^3S_1$ metastable state of He, which is calculated [27]. These results, along with various theoretical calculations [12–19] of the polarizability of sodium, are shown in Fig. 10. Our measurement is consistent with all measurements and theories that quote errors (we note that [17] is aimed primarily at the frequency-dependent polarizability). Even though much more accurate, our result is a general confirmation of the methods used in these calculations as well as a stimulus for theorists to reduce (and to estimate) the errors in future polarizability calculations.

The dramatic increase in accuracy of atomic polarizability achieved here comes from measuring the Stark energy directly rather than its spatial derivative, that is, from measuring a phase shift rather than a deflection. This requires accurate knowledge of a uniform electric field, rather than an electric-field gradient. Previous efforts were limited by the knowledge of the exact value of the gradient and the field at the position of the atomic beam, whether the deflection was measured directly or as a shift of the fringes in a Young's double-slit atom interferometer [5]. An additional advantage of our technique is that diffraction from an accurately fabricated diffraction grating is an excellent method for determining atomic velocity absolutely. Significant improvements in our technique would result from an interaction region whose spacing was determined more accurately (e.g., with light interferometry) and from finding a way to determine the velocity of the interfering atoms (e.g., by a magnetic or radio frequency rephasing experiment [26] or by using pulsed atomic beam techniques [28]). With improvements of this type, it seems feasible to perform polarizability measurements with uncertainties in the 10^{-4} range.

Our sodium polarizability measurement leads to improved accuracy for the value of related polarizabilities. When combined with the measurements of the Stark effect in Na [21,22] more accurate values of the electric polarizabilities of the excited states of the Na atom result: $\alpha(3\,^2P_{3/2})=53.40(11)\times10^{-24}$ cm^3 and $\alpha(3\,^2P_{1/2})$

$=53.23(9)\times10^{-24}$ cm^3. The previous most accurate experimental value of the sodium electric polarizability [10] was based on a measurement relative to the polarizability of the $^3S_1$ metastable state of He that was calculated [27]. Using our measurement together with the experiment [10] allows us to determine the polarizability of the $^3S_1$ metastable state of He to be $47.7(1.0)\times10^{-24}$ cm^3 in good agreement with the calculated value 46.77×10^{-24} cm^3 [27]. The error in the experimental value is dominated by the experiment in Ref. [10].

VI. CONCLUSION

In conclusion, we have demonstrated an atom interferometer with physically separated beams and used it for a measurement of the polarizability of the ground state of sodium. We achieved an uncertainty an order-of-magnitude smaller than the best previous determination of atomic polarizability in any condensable atomic system. Our measurement sets a test for model calculations of multielectron atoms. It would be desirable to apply this technique to cesium as a check on the theories used to extract the Weinberg angle from measurements of parity nonconservation in this system [29]. In addition, atom interferometers with physically separated beams open up the possibility of several other experiments, such as a measurement of the index of refraction of a gas for matter waves [30], a topological measurement of the Aharonov-Casher phase shift, and the measurement of Berry's phase for the wave function of a massive boson [26], which requires the ability to apply uniform, well-controlled interactions to one portion of a split atom wave.

ACKNOWLEDGMENTS

The atom gratings used in this work were made in collaboration with Mike Rooks at the National Nanofabrication Facility at Cornell University [25]. This work was supported by the U.S. Army Research Office Contract Nos. DAAL03-89-K-0082 and ASSERT 29970-PH-AAS, the Office of Naval Research Contract No. N00014-89-J-1207, and the Joint Services Electronics Program Contract No. DAAL03-89-C-0001. T.D.H. acknowledges the support of the National Science Foundation. J.S. acknowledges the support of the Fond zur Förderung der Wissenschaftilchen Forschung in Austria and of the Austrian Academy of Sciences.

[1] O. Carnal and J. Mlynek, Phys. Rev. Lett. **66**, 2689 (1991).
[2] D. W. Keith, C. R. Ekstrom, Q. A. Turchette, and D. E. Pritchard, Phys. Rev. Lett. **66**, 2693 (1991).
[3] F. Riehle, T. Kisters, A. Witte, J. Helmcke, and C. J. Bordé, Phys. Rev. Lett. **67**, 177 (1991).
[4] M. Kasevich and S. Chu, Phys. Rev. Lett. **67**, 181 (1991).
[5] F. Shimizu, K. Shimizu, and H. Takuma, Jpn. J. Appl. Phys. **31**, L436 (1992).
[6] V. Rieger, K. Sengstock, U. Sterr, J. H. Müller, and W. Ertmer, Opt. Commun. **99**, 172 (1993).
[7] *Optics and Interferometry with Atoms,* edited by J. Mlynek, V. Balykin, and P. Meystre, special issue of Appl. Phys. B **54** 321 (1992).
[8] *Matter Wave Interferometry,* edited by G. Badurek, H. Rauch, and A. Zeilinger, special issue of Physica B&C **151**, 1 (1988).
[9] N. F. Ramsey, *Molecular Beams* (Oxford University Press, Oxford, England, 1956).
[10] R. W. Molof, H. L. Schwartz, T. M. Miller, and B. Bederson, Phys. Rev. A **10**, 1131 (1974).
[11] K. D. Bonin and M. A. Kadar-Kallen, Int. J. of Mod. Phys. B **8**, 3313 (1994).
[12] K. T. Tang, J. M. Norbeck, and P. R. Certain, J. Chem. Phys. **64**, 3063 (1976).
[13] E.-A. Reinsch and W. Meyer, Phys. Rev. A **14**, 915 (1976).
[14] P. Fuentealba, J. Phys. B **15**, L555 (1982).
[15] G. S. Soloveva, P. F. Gruzdev, and A. I. Sherstyuk, Opt. Spektrosk. **57**, 776 (1984) [Opt. Spectrosc. (USSR) **57**, 473 (1984)].
[16] W. Müller, J. Flesch, and W. Meyer, J. Chem. Phys. **80**, 3297 (1984).
[17] B. Kundu, D. Ray, and P. K. Mukherjee, Phys. Rev. A **34**, 62 (1986).
[18] Z. Liu, Ph.D. thesis, Notre Dame, 1989 (unpublished).
[19] P. Fuentealba and O. Reyes, J. Phys. B **26**, 2245 (1993).
[20] W. D. Hall and J. C. Zorn, Phys. Rev. A **10**, 1141 (1974).
[21] L. Windholz and C. Neureiter, Phys. Lett. A **109**, 155 (1985).
[22] L. Windholz and M. Musso, Phys. Rev. A **39**, 2472 (1989).
[23] B. J. Chang, R. Alferness, and E. N. Leith, Appl. Opt. **14**, 1592 (1975).
[24] C. R. Ekstrom, Ph.D. thesis, Massachusetts Institute of Technology, 1993 (unpublished).
[25] C. R. Ekstrom, D. W. Keith, and D. E. Pritchard, Appl. Phys. B **54**, 369 (1992).
[26] J. Schmiedmayer, C. R. Ekstrom, M. S. Chapman, T. D. Hammond, and D. E. Pritchard, in *Fundamentals of Quantum Optics III, Küthai, Austria, 1993,* edited by F. Ehlotzky (Springer-Verlag, Berlin, 1993).
[27] K. T. Chung and R. P. Hurst, Phys. Rev. **152**, 35 (1966).
[28] T. D. Hammond, D. E. Pritchard, M. S. Chapman, A. Lenef, and J. Schmiedmayer, in *Fundamental Systems in Quantum Optics,* special issue of Appl. Phys. B **60**, 193 (1995).
[29] M. C. Noecker, B. P. Masterson, and C. E. Wieman, Phys. Rev. Lett. **61**, 310 (1988).
[30] J. Schmiedmayer, M. S. Chapman, C. R. Ekstrom, T. D. Hammond, S. Wehinger, and D. E. Pritchard, Phys. Rev. Lett. **74**, 1903 (1995).

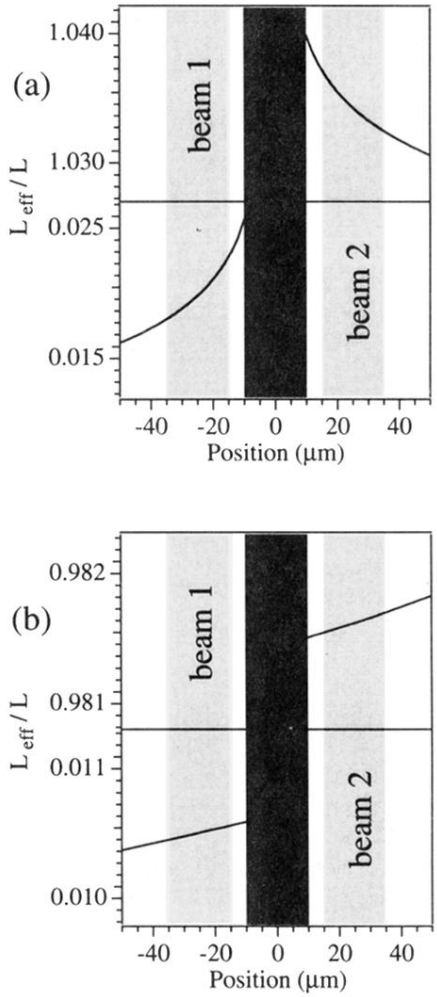

FIG. 6. Calculated values of L_{eff} as a function of distance from the septum (black) for interaction regions (a) without any guard electrodes and (b) with guard electrodes. The gray areas labeled beam 1 and beam 2 show the approximate paths of the two atom beams with respect to the septum. Here, the voltage is applied to the side containing beam 2.